A Valence Force Field for Zirconocene Dichlorides

Udo Höweler,* Roland Mohr, Markus Knickmeier, and Gerhard Erker*

Organisch-Chemisches Institut der Universität Münster, Corrensstrasse 40, D-48149 Münster, Germany

Received February 23, 1994®

In this study valence force field parametrizations for zirconocene dichloride complexes are reported. The three models developed and investigated provide complete sets of parameters that can be used either in standard force fields without software extensions for the treatment of π-ligands or in force fields that can handle the multiple-reference problem encountered in highly symmetric coordination compounds as well as in force fields where a distributed-forces model for the treatment of centrosymmetric ligands is available. The new parameters have been tested with a series of 21 nonbridged and 12 *ansa*-metallocene complexes. The agreement between X-ray structural data and the results of the three model calculations is excellent. On the average, bond lengths are reproduced to better than 2 pm, bond angles to 1°, and the torsion angles defining the relative orientations of the ligands in the bent-metallocene conformers to about 6° for complexes exhibiting no significant intermolecular interaction in the solid state. Additionally, the new series of parameter sets presented allows for a good reproduction of the experimental vibrational data.

Early-transition-metal metallocene complexes are actively being studied as homogeneous catalysts for the stereospecific Ziegler–Natta polymerization of α-olefins. Isotactic polypropylene has been produced using catalysts derived from group IV metallocene dichlorides with methylalumoxane cocatalyst. The catalyst precursors often are of the general form Cp_2ML_2 and consist either of *ansa*-metallocenes or of suitably substituted nonbridged metallocene compounds.[1-3] In the case of C_2-symmetric *ansa*-metallocene dichlorides the transfer of chirality and thus the obtained polymer tacticity in Ziegler–Natta catalysis can be correlated with the structural features at the rigid metallocene framework. For some nonbridged Ziegler-type catalysts it could be shown that, even though they exhibit C_2 symmetry in the solid state, polypropylene of rather low isotacticity is formed because of the existence of C_1-symmetric conformers in solution.[4]

The elucidation of this problem, especially the description of the dynamic behavior of catalyst precursors, can potentially be facilitated by the use of computational methods, namely molecular mechanics methods. Recent reports on the application of molecular mechanics to organometallic compounds concerning studies of cyclopentadienyl complexes have used nonvalence force fields.[5] From early papers trying to rationalize the selectivity of Ziegler–Natta catalysis, it appears that the environment around the metal was forced to be rigid.[6] Corradini[7] and Rappé et al.[8] have used combined ab initio and molecular mechanics methods and fixed the ligand frame in the transition state of the propagation step in Ziegler–Natta catalysis in attempting to rationalize the resulting polypropylene tacticity. Within such topochemical models a reliable structural prediction of unknown metallocene compounds seems to be problematic. Due to the fixation of the ligand frame, steric interactions between substituents and the growing alkyl chain tend to become overestimated in this approach.[6-8] Additionally, with these models a realistic description of the dynamic properties of catalyst precursors is difficult. Attempts in this direction will require the use of algorithms for a general computational treatment of π-ligands, because these systems are difficult to calculate by standard procedures due to their unique coordination symmetry.

To our knowledge the first self-consistent valence force field for metallocenes was recently reported by Landis et al.[9,10] Their derivation was based on the SHAPES extension to the CHARMM force field that uses a Fourier term instead of the harmonic term for bond angle potentials.[11] To us it appeared advantageous to derive an

® Abstract published in *Advance ACS Abstracts*, April 15, 1994.

(1) Sinn, H.; Kaminsky, W. *Adv. Organomet. Chem.* **1980**, *18*, 99. Kaminsky, W.; Kulper, K.; Brintzinger, H. H.; Wild, F. R. W. P. *Angew. Chem.* **1985**, *97*, 507; *Angew. Chem., Int. Ed. Engl.* **1985**, *24*, 507. Ewen, J. A. *J. Am. Chem. Soc.* **1984**, *106*, 6355.

(2) Schnutenhaus, H.; Brintzinger, H. H. *Angew. Chem.* **1979**, *91*, 837; *Angew. Chem., Int. Ed. Engl.* **1979**, *18*, 777. Recent examples: Bandy, J. A.; Green, M. L. H.; Gardiner, I. M.; Prout, K. *J. Chem. Soc., Dalton Trans.* **1991**, 2207. Rheingold, A. L.; Robinson, N. P.; Whelan, J.; Bosnich, B. *Organometallics* **1992**, *11*, 2812. Chen, Z.; Halterman, R. L. *J. Am. Chem. Soc.* **1992**, *114*, 2276. Rieger, B. *J. Organomet. Chem.* **1992**, *428*, C33. Mallin, D. T.; Rausch, M. D.; Lin, Y.-G.; Dong, S.; Chien, J. C. W. *J. Am. Chem. Soc.* **1990**, *112*, 2030. Llinas, G. H.; Dong, S.; Mallin, D. T.; Rausch, M. D.; Lin, Y.-G.; Winter, H. H.; Chien, J. C. W. *Macromolecules* **1992**, *25*, 1242 and literature cited in these references.

(3) Ewen, J. A.; Jones, R. L.; Razavi, A.; Ferrara, J. D. *J. Am. Chem. Soc.* **1989**, *110*, 6255. Ewen, J. A. Catalytic Polymerization of Olefins. Keii, T., Soga, K., Eds.; *Stud. Surf. Sci. Catal.* **1986**, *25*, 271. Ewen, J. A.; Elder, M. J.; Jones, R. L.; Curtis, S.; Chen, H. N. *Stud. Surf. Sci. Catal.* **1990**, *56*, 439 and references cited therein.

(4) Erker, G.; Aulbach, M.; Knickmeier, M.; Wingbermühle, D.; Krüger, C.; Nolte, M.; Werner, S. *J. Am. Chem. Soc.* **1993**, *115*, 4590.

(5) Brubaker, G. R.; Johnson, D. W. *Coord. Chem. Rev.* **1984**, *53*, 1. Buckingham, D. A.; Maxwell, I. E.; Sargeson, A. M.; Snow, M. R. *J. Am. Chem. Soc.* **1970**, *92*, 3617. Hambley, T. W. *Inorg. Chem.* **1988**, *27*, 2496.

(6) Kamamura-Kuribayshi, H.; Koga, N.; Morokuma, K. *J. Am. Chem. Soc.* **1992**, *114*, 8687.

(7) Corradini, P.; Barone, V.; Fusco, R.; Guerra, G. *J. Catal.* **1982**, *77*, 32. Corradini, P.; Guerra, G.; Pucciariello, R. *Macromolecules* **1985**, *18*, 2030. Venditto, V.; Guerra, G.; Corradini, P. *Eur. Polym. J.* **1991**, *27*, 45–54. Venditto, V.; Guerra, G.; Corradini, P.; Fusco, R. *Polymer* **1991**, *32*, 1329. Cavallo, L.; Corradini, P.; Guerra, G.; Vacatello, M. *Polymer* **1991**, *32*, 1329. Cavallo, L.; Guerra, G.; Vacatello, M.; Corradini, P. *Macromolecules* **1991**, *24*, 1784.

(8) Castonguay, L. A.; Rappé, A. K. *J. Am. Chem. Soc.* **1992**, *114*, 5832.

(9) Doman, T. N.; Landis, C. L.; Bosnich, B. *J. Am. Chem. Soc.* **1992**, *114*, 7264.

(10) Hollis, T. K.; Burdett, J. K.; Bosnich, B. *Organometallics* **1993**, *12*, 3385.

(11) Allured, V. S.; Kelly, C. M.; Landis, C. R. *J. Am. Chem. Soc.* **1991**, *113*, 1.

0276-7333/94/2313-2380$04.50/0

algorithm of the valence force field of π-ligands and coordinated metal centers that can be applied within the majority of the commercially available force field program packages without the necessity of changing the computational routines. In order to allow future advanced studies on the dynamic features of Ziegler–Natta catalyst systems, the parameter set chosen must reproduce the experimental IR frequencies of the zirconocene dichloride complexes well. Only then can a realistic overall force field description of the complexes be anticipated. In this paper we present three independent models for describing π-ligands which we have developed with these presumptions. The performance of two of these models is compared with the results of the distributed-force approach by Landis et al.[9] We especially address the question whether artificially high force constants are really needed for coupling the π-system to the metal center.

This new force field development for zirconocene dichlorides should be helpful to elucidate, for example, the stereoselectivity of α-olefin polymerization processes in a very realistic manner with relaxed transition states using combined ab initio and molecular mechanics methods.

Results and Discussion

Force Field Description of π-Complexes. The force field treatment of π-complexes requires a model suited to describe the essential metal–π-system interaction. Struchkov et al.[12] have proposed a very simple and intuitive model for the bonding framework of π-systems coordinated to metal atoms. According to this model the metal–π-ligand interaction is simulated by an artificial bond between the metal atom and a dummy atom (MP) located in the center of the π-system. Thus, in this model only one set of bond lengths, bond angles, and torsional parameters is needed to describe the geometry and energy of the metal–ligand π-interaction and also ring tilting as well as rotation of the π-ligand about the metal–centroid axis, respectively.

The additional center MP introduces artificial force field potentials for the bonds from the ring carbons (5C) to the MP and for the 5C–MP–5C angles into the structural model. While the first can easily be dealt with by taking the distance of the midpoint to a ring atom as the reference value for the bond length, the corresponding angles lead to a multiple-reference problem (unique-labeling problem[11]) because equilibrium values of 72 and 144° are found for these angles (e.g. 1–MP–2 = 72°, 1–MP–3 = 144°; formula I). Thus, the 5C–MP–5C bond angle is uniquely

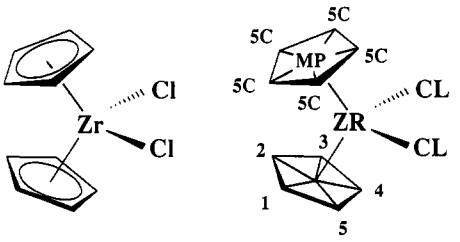

I

defined only when different center types (labels) are assigned to each of the ring atoms. Landis et al.[11] have proposed a Fourier angular potential to handle the multiple-reference problem. Here we will use a different approach based on a set of harmonic potentials common to standard force fields such as TRIPOS,[13] CHARMM,[14] and AMBER.[15]

The algorithm is implemented[16] in MOBY 1.5, the molecular modeling program[17] we have used for this study, as follows: (i) for every three centers constituting a bond angle, several reference values and their corresponding force constants can be provided; (ii) prior to a single energy calculation or an optimization the program chooses the reference value which is closest to the current value of the bond angle;[16] (iii) this reference value and the force constant are then retained throughout the optimizations and energy calculation process. Thus, only a single harmonic term is calculated for each bond angle but the reference values and force constants are assigned such as to minimize the potential in the starting geometry. The advantages of this approach are obvious: (i) it solves the unique-labeling problem because no artificial assignment of different types of centers to chemically equivalent atoms is necessary; (ii) different force constants can be applied to mimic harder or softer potentials for specific bond angles; (iii) zero-potential energies are calculated for idealized geometries.

For cyclopentadienyl ring systems reference values α = 72° and β = 144° for the 5C–MP–5C bond angles in the π-ligands have to be specified, while the values α = 60°, β = 120°, and γ = 180° are needed for six-membered rings in order to calculate zero-potential energies for idealized geometries:

II

Landis et al. have discussed the necessity of deriving new algebraic formulas for the valence force field terms of metal atoms[11] due to the broader range of bond angles (i.e. softer potentials) at the metal atoms. In the X-ray structures of the zirconocene dichlorides discussed here, the environment around the zirconium center is rather rigid with bond angles within a range of ±5° about the average value. Thus, the standard harmonic term can be applied without disadvantage.

Landis et al. have proposed a special treatment of the dummy atom (MP) inside the π-ligand.[9] They have introduced the dummy atom dynamically by redefining its position prior to each energy and gradient calculation as the center of the π-system. The forces exerted on the dummy atom are then distributed to the ring carbon atoms. Thus, the dummy atom is not explicitly a part of the structure. These authors rationalize this procedure as follows: (i) high force constants would be necessary to couple the ring carbon centers to the movement of the

(12) Timofeera, T. V.; Solovokhotov, Y. L.; Struchkov, Y. T. *Dokl. Akad. Nauk SSSR* **1987**, *294*, 1173.

(13) Clark, M.; Cramer, R. D., III; Van Opdenbusch, N. *J. Comput. Chem.* **1989**, *10*, 982.

(14) Brooks, R. B.; Bruccoleri, R. E.; Olafson, B. D.; States, D. J.; Swaminathan, S.; Karplus, M. *J. Comput. Chem.* **1993**, *4*, 187.

(15) Weiner, S. J.; Kollman, P. A.; Case, A. D.; Chandra Singh, U.; Ghio, C.; Allagona, G.; Profeta, S., Jr.; Weiner, P. *J. Am. Chem. Soc.* **1984**, *106*, 765.

(16) Wiesemann, F.; Teipel, S.; Krebs, B.; Höweler, U. *Inorg. Chem.*, in press.

(17) Höweler, U. *MOBY 1.5, Molecular Modelling on the PC*; Springer-Verlag: Heidelberg, Germany, 1992.

respective dummy atom; (ii) since the dummy atom is not part of the structure, no spurious vibrations are found in the IR spectra of the complexes and the frequencies for the actual vibrations of the molecule are not affected by any vibrations involving the dummy atom.

Since specific potential functions or algorithms for the force field treatment of metal centers may not be available in every modeling program, we have developed three different model types. The impact of the different approaches on the quality and reliability of the static and dynamic properties is investigated for the zirconocene dichlorides. The parameters developed for model 1 can be used in every force field, while model 2 can only be applied if a multiple-reference algorithm is available. Model 3 is equivalent to the approach used by Landis et al.[9] for the calculation of ferrocenes and ruthenocenes in their extended version of the CHARMM force field.

For these models several universal parameters are provided that are always treated in the same manner, angular terms (Θ_1, 5C–MP–Zr; Θ_2, MP–Zr–MP) and torsion terms (Φ, 5C–MP–Zr–MP), for the description of the zirconium environment:

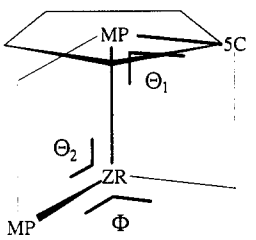

III

Specific variations are then made within each of the three model types. These are described as follows.

Model 1 (for Standard Force Fields without Extensions). With every standard force field enabled to handle up to six bonds for a single center, the special case of the multiple-reference problem encountered with π-ligands can be solved by using a zero force constant for the 5C–MP–5C bond angle:

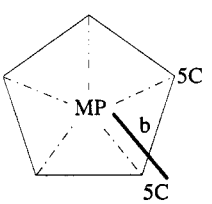

$V_{b(MP\text{-}5C)} = k_b(b-b^0)^2$

$V_{ang(5C\text{–}MP\text{–}5C)} = 0$

IV

This is sufficient to avoid artificial energy contributions and forces that are introduced by inappropriate reference values. In this approach coupling of the dummy atom to the ring is described by the force constant of the bond length term V_b(MP–5C) only. Thus, a total of five bond length potentials are calculated in order to locate the dummy atom at the center of the ring.

Model 2 (for Force Fields with a Multiple Reference Algorithm). Coupling of the dummy atom to the ring can alternatively be simulated by an appropriate combination of bond length and bond angle potentials. We have used a bond angle potential consisting of the two possible references (φ = 72° or φ = 144°):

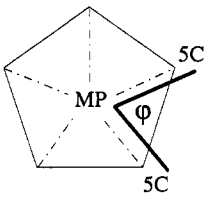

$V_{b(MP\text{-}5C)} = 0$

$V_{ang(5C\text{–}MP\text{–}5C)} = k_\varphi(\varphi-72°)^2$

$V_{ang(5C\text{–}MP\text{–}5C)} = k_\varphi(\varphi-144°)^2$

V

The force constants for the bond length potentials were set to zero, and the coupling of the π-ligand to the metal center is effected by the 10 bond angle terms only.

Model 3 (for Force Fields with a Distributed Forces Algorithm). In contrast to the other models presented, in model 3 the dummy atom is not treated like a real structural element but, rather, like a virtual atom:

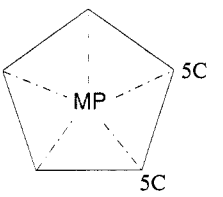

$V_{b(MP\text{-}5C)} = 0$

$V_{ang(5C\text{–}MP\text{–}5C)} = 0$

MP : virtual atom

VI

This approach of Landis et al.[9] was implemented in the following way: (i) the dummy atoms are positioned at the center of the π-systems; (ii) these atoms are marked for the dynamic repositioning and are not included in the optimization; (iii) prior to every energy calculation these atoms are recentered; (iv) the energy contributions due to the valence force field terms are added to the total energy; (v) in the gradient calculations the gradient components of these dummy atoms are distributed to the centers of the ring. The Cartesian coordinates α_{MP} ($\alpha = x, y, z$) of the dummy atom are defined by the coordinates of the atoms in the n-membered ring:

$$\alpha_{MP} = \frac{1}{n}\sum_{i=1}^{n}\alpha_i$$

Thus, any Cartesian gradient component for the dummy atom is transferred to the ring atoms by application of the chain rule:

$$\frac{\partial V}{\partial \alpha_i} = \frac{\partial V}{\partial \alpha_{MP}}\frac{\partial \alpha_{MP}}{\partial \alpha_i}$$

This means that the forces exerted on the dummy atom are distributed to the centers of the ring.

Force Field. We have employed the PC-based molecular modeling program MOBY 1.5[17] for the generation of the initial starting structures and for the visualization and analysis of the optimized molecular geometries. The geometry optimizations and vibrational analyses were carried out with the batch-oriented version of MAXIMOBY 3.1[18] run either on a PC or an IBM RS6000-32H workstation. The MOBY implementation of the AMBER force field functions[15] was used with the necessary modifications for the treatment of the metal coordination shell as described below.

(18) Höweler, U. *MAXIMOBY 3.1*; CHEOPS: Münster, Germany, 1992.
(19) Broyden, C. G. *Math. Comput.* **1967**, *21*, 368. Fletscher, R. *Comput. J.* **1970**, *13*, 371. Goldfab, D. *Math. Comput.* **1970**, *24*, 23. Shanno, D. F. *Math. Comput.* **1970**, *24*, 647.

In the AMBER force field the valence contributions V_{val} to the force field energy V_{tot} consist of harmonic terms for bond lengths and bond angles and Fourier terms for the torsional and improper torsional potentials:

$$V_{val} = V_{bond} + V_{ang} + V_{tor} + V_{imp}$$

$$V_{bond} = \sum_b k_b(b - b^0)^2$$

$$V_{ang} = \sum_\varphi k_\varphi(\varphi - \varphi^0)^2$$

$$V_{tor} = \sum_\phi V_\phi(1 + \cos(n\phi - \phi^0))$$

$$V_{imp} = \sum_{imp} V_{imp}(1 + \cos(2\phi - 180°))$$

The harmonic potentials are defined by the force constants k_b and k_φ for the bond length and bond angle functions, respectively, and their corresponding reference values b^0 and φ^0. These parameters are determined to reproduce experimental data for the corresponding geometry parameters. The V_ϕ amplitudes of the torsion terms are chosen to reproduce the height of the experimental torsional barrier for the bond, while the multiplicity n reflects the periodicity of the torsional potential and the shift ϕ^0 determines the minimum energy torsion angle. Improper torsion terms have only been used to ensure the planarity of the sp^2-hybridized carbon centers in the aromatic substituents but not for the centers in the π-ligand itself. A Fourier term is applied to these improper torsions, where the torsion angle is defined by the sp^2 center and its three bonded neighbors.

Since the molecules used in this study do not contain polar groups, we have omitted the Coulomb term of the force field. Landis et al.[9] had pointed out that electrostatic interactions contributed significantly to the total energy of the ferrocenes but were not important for the relative energies of their respective conformers. Since acidic hydrogens are also not present in the complexes investigated during this study, the specific hydrogen-bonding term of the AMBER force field was also not needed. Thus, the nonvalence contribution V_{nonval} is given by the van der Waals term only. This term is calculated by a Lennard–Jones 12–6 potential for atoms i and j separated by at least three bonds

$$V_{nonval} = V_{vdW} = \sum_{i<j} \epsilon_{ij}\left(\left(\frac{\sigma_{ij}}{r_{ij}}\right)^{12} - 2\left(\frac{\sigma_{ij}}{r_{ij}}\right)^{6}\right)$$

with the usual definition of the mixed atom parameters

$$\epsilon_{ij} = (\epsilon_{ii}\cdot\epsilon_{jj})^{1/2}$$

$$\sigma_{ij} = \frac{1}{2}(\sigma_{ii} + \sigma_{jj})$$

The generalized center types[17] have been assigned to all atoms in the examples looked at in this study, except for those that will be discussed specially below. Thus, those parts of the molecules that are not connected to the Zr atom by a valence force field term are described with the same parameter set used in ordinary organic compounds. The additional parameters needed for the Zr environment were derived by the normal-coordinate analysis of Cp_2ZrCl_2 reported below.

Table 1. Parameters for the Additional Center Types in the MOBY Force Field

center type	atomic no.	atomic mass (au)	vdW radius (Å)	well depth (kcal/mol)	valency	descripn
ZR	40	91.2	1.80	0.05	4	metal atom
MP	99	12.0[a]	0.10	0.00	6[b]	π-ligand centroid
5C	6	12.0	1.85	0.12	4	C in cp ring
ZC	6	12.0	1.85	0.12	4	C at junction between 5- and 6-rings

[a] This mass is used in models 1 and 2 only. [b] Minimum number of bonds for the Struchkov model for π-ligands.[12]

The additional center types introduced to describe the metal atom and the π-system are

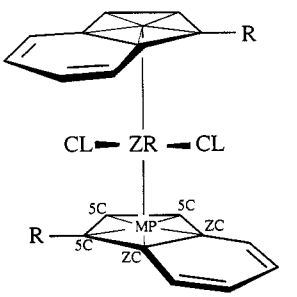

VII

ZR stands for the metal atom itself, the dummy atom MP denotes the center of the ring, 5C stands for the centers in the cyclopentadienyl and tetrahydroindenyl ligands, and ZC denotes those centers shared by the five- and six-membered rings in the indenyl ligands. The atomic parameters for the generalized sp^2-hybridized carbon (2C) in MOBY were used for the atoms in the π-system, but no improper torsional term was calculated for these centers. Table 1 summarizes the new types of centers and their atomic parameters. The van der Waals radius for Zr appears more appropriate for a neutral zirconium atom than for a zirconium ion with a formal partial charge of +2. However, we decided to use this value because the formal +2 charge is significantly reduced by delocalization of the electrons from the π-systems to the metal atom. No changes in the geometries of the complexes could be determined when smaller values are used for the Zr atomic radius.

Optimization Procedure. The following procedure was applied to obtain the minimum energy structures for all 33 complexes studied. For each example all optimizations were run for each of the three models. The experimental structures obtained by X-ray diffraction were taken as the starting geometries (Schemes 1 and 2). MOBY was used to assign the types of centers, to add the hydrogen atoms, and to construct the dummy atoms at the center of the rings. The parameter set was tested for completeness, and the geometry was stored in a MOBY library for subsequent calculations with MAXIMOBY.

Prior to the optimizations every atom was displaced by 0.1 Å, randomly distributed over its Cartesian components to reduce the symmetry of the starting structure. Then, four optimization steps were run using the conjugate gradient (CG) method and the BFGS[18] implementation with increasing convergence criteria on the change of the total energy (CG, 10^{-4} kcal/mol; BFGS, 10^{-5} kcal/mol; CG, 10^{-6}/BFGS, 10^{-20} kcal/mol). This procedure leads to

Scheme 1. Structures of Nonbridged Zirconocene Dichlorides Used in the Force Field Calculations (● = Zr, ○ = Cl)[30]

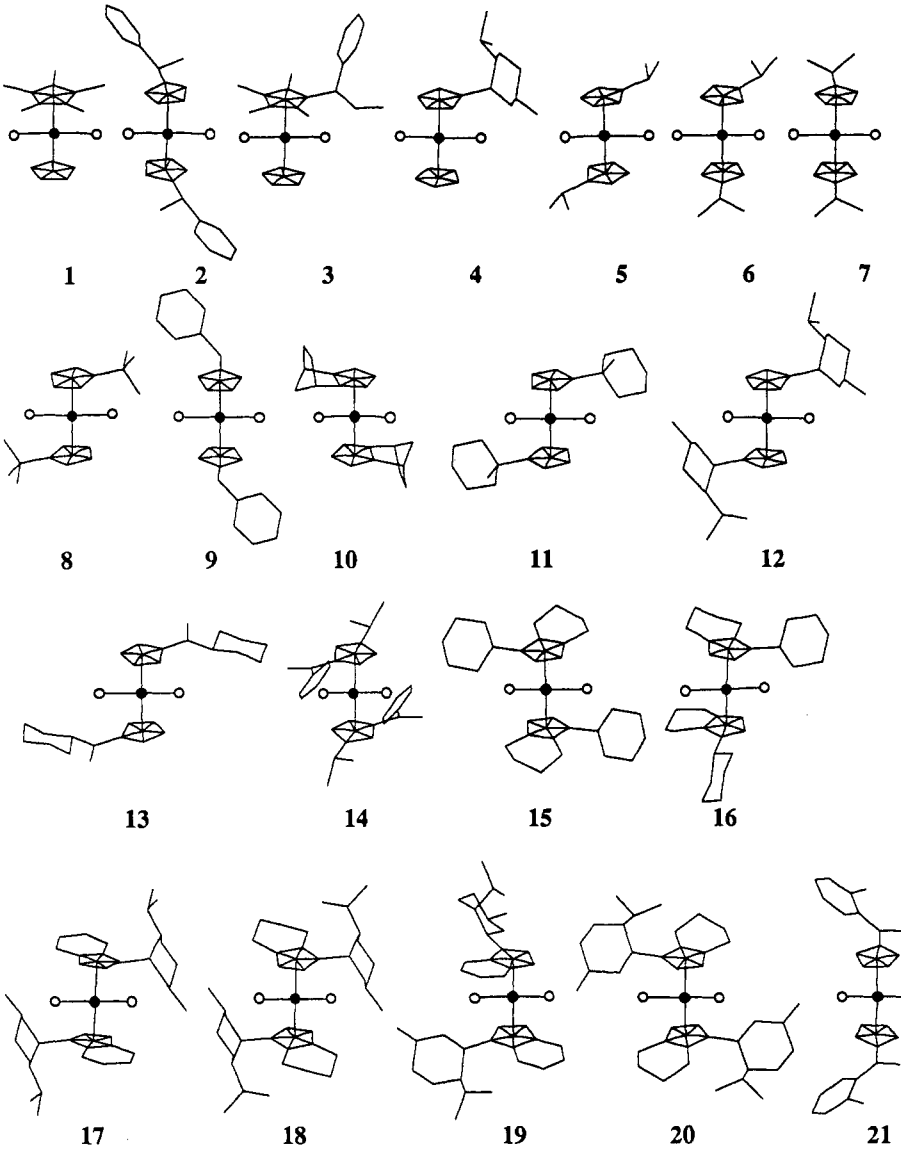

Scheme 2. Structures of *ansa*-Zirconocene Dichlorides Used in Force Field Calculations (● = Zr, ○ = Cl)[31]

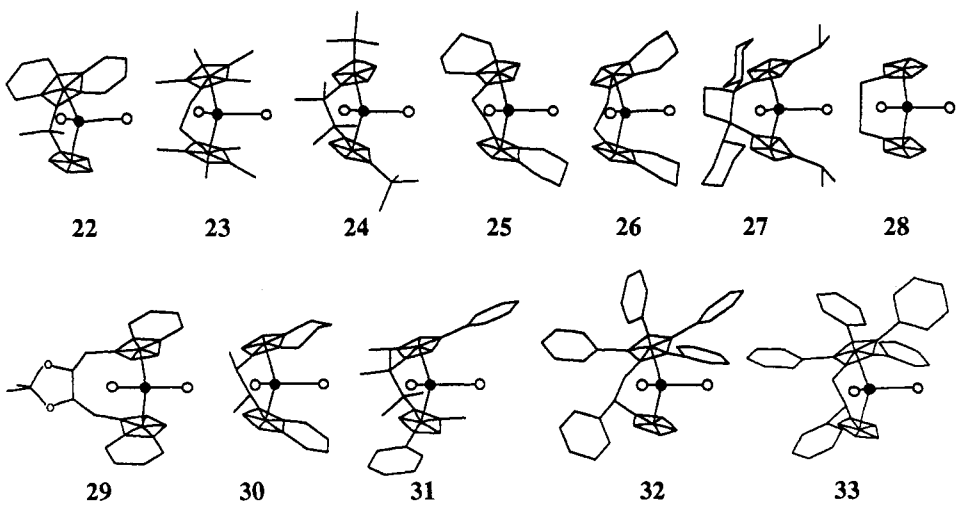

stationary points with RMS gradients below the threshold of 10^{-3} kcal/(mol Å).

Finally, the minimum finder was envoked to ensure convergence to a local minimum. The minimum finder consists of an optimization step followed by a normal-coordinate analysis. Whenever imaginary frequencies are obtained for the nontrivial vibrations, the geometry is changed along the normal coordinate corresponding to

Table 2. Parameters for Additional Force Field Terms

geometrical param[a]	force constant amplitude model 1	model 2	model 3	ref value/shift	multiplicity
		Bonds[b]			
ZR–CL	120	120	110	2.44	
ZR–MP	250	250	140	2.20	
MP–5C	30	0	0	1.19	
5C–5C	400	400	400	1.40	
HC–5C	370	370	370	1.08	
3C–5C	320	320	320	1.52	
		Angles[c]			
CL–ZR–CL	80	80	80	97.2	
MP–ZR–CL	80	80	80	106	
5C–MP–5C	0	10	0	72	
	0	10	0	144	
ZR–MP–5C	120	100	60	90	
5C–5C–5C	100	100	100	108	
5C–5C–HC	30	30	30	126	
5C–5C–2C	85	85	85	126	
5C–5C–3C	70	70	70	126	
5C–ZC–2C	70	70	70	132	
5C–ZC–3C	70	70	70	130	
ZC–ZC–3C	70	70	70	120	
HC–5C–MP	0	0	0	180	
		Torsions[c]			
- - -Zr–MP- - -	0	0	0	180	5
- - -MP–5C- - -	0	0	0	0	0
- - -5C–2C- - -	1	1	1	180	2
- - -5C–3C- - -	0	0	0	180	3
- - -5C–5C- - -	0.50	0.50	0.50	180	2
MP–ZR–MP–5C	0.05	0.05	0.05	180	10
5C–5C–5C–5C	6	6	6	180	2
HC–5C–5C–HC	4	4	4	180	2

[a] ZC = 5C, except for the parameters given. [b] Force constant amplitudes in kcal/(mol Å) and reference values in Å. [c] Force constant amplitudes in kcal/(mol rad) and reference values in degrees.

the largest imaginary frequency until a decrease in energy is calculated. The resultant geometry is then reoptimized. This procedure is rerun until no imaginary frequency is found for the nontrivial vibrations. Thus, all resultant geometries are characterized as local minima. The results of the final vibrational analysis were stored for later comparison of low-frequency modes and geometry changes during the optimization.

Conformation analyses were run for both Zr–MP bonds in the open complexes (Scheme 1). The torsion angles were changed by 15° steps for 360°, and all conformers were optimized to the same accuracy as the original structures. In every case four distinct minima (three if a pair of identical ligands is present) could be located with central/central, central/lateral, lateral/central, or lateral/lateral orientation of the substituents at the cyclopentadienyl rings. The energy differences of these respective conformers were found to be less than 2 kcal/mol for the examples investigated. In the meso isomers of the indenyl and tetrahydroindenyl complexes (**16**, **25**) only very shallow minima were found for the lateral positions of the indenyl-type substituents. Details on the conformation analysis together with a discussion of related low-temperature NMR studies will be discussed in a separate paper.[20]

Vibrational Analysis of the Zirconocene Dichlorides. The three models were employed to calculate the vibrational spectra of the parent compound, the unsubstituted zirconocene dichloride. The experimental structure of Cp_2ZrCl_2[21] was used as the starting point for a full geometry optimization employing the procedure outlined above. The mass-weighted Hessian was calculated on the basis of the Cartesian displacement coordinates and transformed to the orthogonal basis as described by Klessinger et al.[22] to separate the translational and rotational degrees of freedom. The diagonalization provides the frequencies and normal coordinates that could easily be related to the results of the vibrational analysis of Cp_2ZrCl_2.[23,24,32]

Table 3. Experimental[23,24,32] and Calculated Vibrational Frequencies (cm^{-1}) for Cp_2ZrCl_2[a]

vibration	exptl value	model 1	model 2	model 3
rotation sym		49	49	49
rotation asym		65	65	65
Cl–Zr–Cl sym	123	140	142	141
Cl–Zr–Cl asym	165	144	145	152
Cp–Zr–Cl sym	140	150	152	157
Cp–Zr–Cl asym	154	162	162	169
Cp–Zr–Cp sym	165	172	173	176
Zr–MP sym	358	260	252	251
tilt asym	266	280	277	268
tilt sym	266	283	276	270
tilt sym	310	292	287	280
tilt asym	310	300	292	283
Zr–Cl asym	333	357	350	365
Zr–Cl sym	333	364	355	361
Zr–MP asym	358	351	344	359
MP in ring		*606*	*600*	
MP in ring		*606*	*603*	
CCCC oop (4)[b]		620	605	569
MP in ring		*644*	*637*	
MP in ring		*661*	*656*	
CCH oop asym		741	741	744
CCH oop sym		745	745	747
CCC inp (4)[b]		839	823	815
CCC oop (4)[b]	840	858	852	842
CCH oop (4)[b]	851	880	873	857
CCH inp (4)[b]	1022	978	972	970
ring breath sym	1125	1022	996	996
ring breath asym		*1023*	996	996
CCH inp (4)[b]		1053	1053	1051
Zr–MP valence sym		*1201*	*1132*	
Zr–MP valence asym		*1212*	*1146*	
CCH inp sym		1256	1256	1256
CCH inp asym		1257	1257	1257
CC valence (4)[b]	1443	1484	1492	1479
CC valence + CCC inp (4)[b]	1368	1580	1593	1577
CH valence (10)[b]	3108	3087	3086	3086

[a] Numbers written in italics correspond to the spurious vibrations involving the dummy atom in the ring. Legend: sym, symmetric; asym, asymmetric; inp, in plane; oop, out of plane. [b] Nearly degenerate vibrations ($\Delta\nu \leq 2$ cm^{-1}); the number indicates the degree of degeneracy.

The force constants were subsequently adjusted for a better fit of the experimental frequencies, and the procedure was repeated until a final set of parameters was obtained. The resultant reference values and force constants are compiled in Table 2. The final frequencies are listed in Table 3 together with the experimental assignments. For models 1 and 2 spurious vibrations are found that involve some movement of the dummy atom. These frequencies are marked in Table 3.

The results are given for the conformation of Cp_2ZrCl_2 lowest in energy, which exhibits the staggered orientation of the rings. Since this geometry has only C_s symmetry

(20) Knickmeier, M.; Sarter, C.; Erker, G. Manuscript in preparation.
(21) Prout, K.; Cameron, T. S.; Forder, R. A.; Crithley, S. R.; Denton, B.; Rees, G. V. *Acta Crystallogr.* **1974**, *B30*, 2290.
(22) Klessinger; M., Pötter, T.; van Wüllen, C. *Theor. Chim. Acta* **1991**, *80*, 1.
(23) Druce, P. M.; Kingston, B. M.; Lappert, M. F.; Srivastava, R. C.; Frazer, M. J.; Newton, W. E. *J. Chem. Soc. A* **1969**, 2814. See also: Wailes, P. C.; Coutts, R. S. P.; Weigold, H. *Organometallic Chemistry of Titanium, Zirconium, and Hafnium*; Academic Press: New York, 1974; p 124.
(24) Samuel, E.; Ferner, F.; Bigorgne, M. *Inorg. Chem.* **1973**, *12*, 881.

with a plane of symmetry passing through MP–Zr–MP, labels are added to indicate the relative ring movement (sym, in phase; asym out of phase) whenever possible.

Simulated spectra obtained from applying all three models are comparable in quality. The dummy atom vibrations in models 1 and 2 are easily discernible because they do not mix with the real vibrations of the molecule. Since several vibrations were not assigned in the vibrational analysis of the experimental data, the comparison of calculated and observed frequencies is incomplete for the vibrations below 100 cm^{-1} and at 560, 1000, and 1260 cm^{-1}. The similarity between the vibrations in ferrocene, for which a complete analysis is available,[9,25] and those of the zirconocene dichloride supports the labeling given in Table 3.

Lappert et al.[23] and Samuel et al.[24] have assigned the single band at 358 cm^{-1} of the experimental spectra to both ring–Zr (symmetric and antisymmetric) vibrations. However, for every ZR–MP force constant in the reasonable range from 50 to 300 kcal/(mol Å) our force field calculations yield a separation of these two modes. On the basis of the resultant parameters (140 kcal/(mol Å) cf. Table 2) the symmetric vibration is located at 251 cm^{-1} and the antisymmetric stretch at 362 cm^{-1} (model 3).

The largest deviation between calculated and observed frequencies (ca. 210 cm^{-1}) is found for the in-plane ring deformation that is observed at 1368 cm^{-1}, while the three models yield values of 1579, 1592, and 1576 cm^{-1}, respectively. This vibration involves a significant coupling of angle-bending and bond-stretching contributions and is therefore difficult to reproduce with a force field that does not explicitly contain these coupling terms. A similar discrepancy was found by Landis et al. in their analysis of the ferrocene vibrational spectra.[9] As in this study, they also calculated the ring-breathing vibration at about 1000 cm^{-1}, which was observed experimentally at 1125 cm^{-1}.

The two rotational modes for the π-ligands about the Zr–MP bond are lowest in energy at 50 and 65 cm^{-1}, respectively, indicating the flexibility of the relative orientations of the π-systems about their minimum energy conformations.

The resultant additional parameter values are summarized in Table 2. The parameters for models 1 and 2 are identical except for the different treatment of the dummy-ring coupling. In either case the force constants for the MP–5C bond (30 kcal/(mol Å)) and the 5C–MP–5C bond angle (10 kcal/(mol rad)) are rather small. Thus, only weak energy terms are introduced for the ligand to metal coupling. In model 3 the optimum values for the Zr–Cl and Zr–MP bonds are significantly lower. The bond angle potentials at the Zr atom are also slightly softer. Thus, the inclusion of an explicit dummy atom to mediate the Zr–ring interaction needs higher forces to induce the ring movement. Still, the force constants required to reproduce the structures and the vibrational spectra for the zirconocene dichlorides are only slightly higher than those for the model of distributed forces that does not contain the dummy atom explicitly.

All three models lead to an optimized structure for Cp_2ZrCl_2 with a relative orientation of the π-ligands intermediate between a staggered and an eclipsed conformation. The van der Waals interaction between the hydrogen atoms of the two rings at the back side of the molecule causes some repulsive potential for both conformations. We have introduced a 10-fold potential for the MP′–Zr–MP–5C torsion about the Zr–MP bond to make the ideal staggered and eclipsed conformations minima of the force field energy. The amplitude for this torsional term is very small, with a rotation barrier of only 0.05 kcal/mol. The energy for the staggered conformer is only slightly lower (0.02 kcal/mol) than for the eclipsed conformer.

Optimized Structures of Cp-Substituted Zirconocene Dichloride Complexes. The series of compounds investigated as typical examples covers nonbridged structures with cyclopentadienyl, indenyl, and tetrahydroindenyl ligands containing one to five substituents (Scheme 1) and bridged structures with one to four carbon atoms connecting the π-ligands (Scheme 2). All examples exhibit η^5-coordination of the π-ligands that allows us to apply our models for the treatment of the bonding frame. In every case a minimum-energy structure could be determined that is close to the X-ray geometry.

In general all geometries are described very well. Tables 4–7 compile the detailed data for the bond lengths and bond angles at the Zr center. In Table 8 a comparison of the three torsion angles is given that describes the orientation of the π-ligand rings. No significant differences between the results from the three models can be found.

In the X-ray structures (Tables 4–7) the various Zr–Cl and Zr–MP bond lengths differ by 2 pm at the most and the Cl–Zr–Cl bond angles vary from 94 to 100° while the MP–Zr–MP angles vary from 118 to 133°. The optimized structures reproduce these features to better than 1.5 pm and 1°. The data for the optimized structures are given as deviations from the X-ray values. A negative entry denotes a smaller bond length or bond angle obtained from the force field optimization.

The relative orientation of the π-systems can best be described by the three torsion angles given in formula VIII and in Table 8. The angle S1 (S–MP–Zr–MP′) denotes

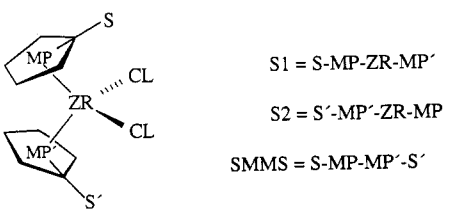

VIII

the rotation for the "upper" ring system (see Schemes 1 and 2), while S2 (MP–Zr–MP–S′) specifies the rotation for the "lower" ring. The relative positions of the substituents are given by the angle SMMS (S–MP–MP′–S′) about the direction from the dummy atom in the upper ring to the dummy atom in the lower ring. For those substituents that are bonded to the π-system by a single connecting bond, S(S′) denotes the ring center that carries the substituent, whereas in the presence of annulated rings (Scheme 1, structure **10**) S (S′) is defined as the midpoint of the bond shared by the two rings. Within this definition torsion angles of ±(150–180)° correspond to the central positioning of the substituents at the front sector of the bent-metallocene unit, whereas angles of ±(70–100)° represent lateral orientations of the substituent.

Again, the torsion angles in the optimized geometries are specified as deviations from the X-ray values. Differences that increase the value of the torsion angle indicate that the substituent is rotated toward the central position,

(25) Bodenheimer, J. S.; Low, W. *Spectrochim. Acta* **1973**, *29A*, 1733.

Table 4. Zr–Cl Bond Lengths and Their Deviations in the Optimized Geometries

structure	X-ray value (pm)	Δ (pm) model 1	Δ (pm) model 2	Δ (pm) model 3
1	244.2	0.1	0.1	0.2
	244.2	0.1	0.1	0.1
2	246.2	−1.9	−1.9	−1.8
	245.5	−1.2	−1.2	−1.2
3	244.3	0.0	0.0	0.0
	243.8	0.5	0.5	0.5
4	243.6	0.8	0.8	0.8
	243.9	0.4	0.4	0.4
5	244.2	0.0	0.0	0.0
	244.2	0.0	0.0	0.0
6	244.9	−0.6	−0.6	−0.6
	244.9	−0.7	−0.7	−0.7
7	244.7	−0.5	−0.5	−0.5
	244.7	−0.5	−0.5	−0.5
8	245.7	−1.6	−1.6	−1.5
	245.7	−1.6	−1.6	−1.5
9	246.2	−1.9	−1.9	−1.9
	246.2	−1.9	−1.9	−1.9
10	244.3	−0.2	−0.2	−0.1
	242.3	1.9	1.9	1.9
11	245.7	−1.6	−1.6	−1.6
	245.7	−1.6	−1.6	−1.6
12	245.1	−0.7	−0.7	−0.6
	245.0	−0.6	−0.6	−0.5
13	243.7	0.5	0.5	0.6
	243.7	0.5	0.5	0.6
14	243.1	1.3	1.3	1.3
	243.2	1.2	1.2	1.3
15	244.2	−0.1	−0.1	−0.1
	244.2	−0.1	−0.1	−0.1
16	244.5	0.1	0.1	0.2
	243.2	1.0	1.0	1.0
17	243.4	1.3	1.3	1.3
	245.3	−0.6	−0.6	−0.6
18	244.1	0.2	0.2	0.2
	244.3	0.2	0.2	0.2
19	240.9	3.3	3.3	3.4
	244.1	0.1	0.1	0.1
20	244.6	0.4	0.4	0.4
	245.1	−1.1	−1.1	−1.1
21	244.4	−0.3	−0.3	−0.2
	244.0	0.3	0.3	−0.5
22	242.1	2.1	2.1	1.9
	242.5	1.5	1.5	1.6
23	244.1	0.1	0.1	0.2
	244.1	0.1	0.1	0.2
24	244.8	−0.8	−0.8	−0.7
	244.8	−1.0	−1.0	−1.1
25	243.8	0.2	0.2	0.2
	243.8	0.2	0.2	0.2
26	242.1	1.7	1.7	1.7
	245.7	−1.5	−1.5	−1.5
27	242.7	1.4	1.4	1.4
	244.5	−0.4	−0.4	−0.3
28	246.1	−1.8	−1.8	−1.8
	243.9	0.3	0.3	0.3
29	243.2	1.2	1.2	1.3
	243.0	1.5	1.5	1.6
30	245.7	−1.5	−1.5	−1.5
	242.6	1.2	1.2	1.1
31	244.6	−0.3	−0.3	−0.2
	244.2	0.2	0.2	0.2
32	242.9	0.7	0.7	0.8
	242.9	1.6	1.6	1.6
33	242.1	2.4	2.4	2.4
	242.9	0.8	0.8	0.9

Table 5. Experimental Zr–MP Bond Lengths and Deviations Obtained in the Force Field Calculations

structure	X-ray value (pm)	Δ (pm) model 1	Δ (pm) model 2	Δ (pm) model 3
1	220.9	0.0	0.0	0.5
	221.9	−0.5	−0.5	0.3
2	217.5	2.9	2.9	3.2
	224.9	−4.0	−4.1	−3.8
3	222.8	−1.1	−1.1	0.1
	221.5	−0.6	−0.6	0.0
4	221.0	−0.4	−0.4	0.0
	219.3	1.6	1.5	2.1
5	221.5	−0.6	−0.6	0.1
	221.5	−0.6	−0.6	0.1
6	220.2	0.5	0.4	0.9
	221.0	−0.1	−0.1	0.5
7	219.9	0.8	0.7	1.2
	219.9	0.8	0.7	1.2
8	221.8	−0.6	−0.7	0.2
	221.8	−0.6	−0.7	0.2
9	217.5	3.0	3.0	3.4
	217.5	3.0	3.0	3.4
10	219.8	0.5	0.5	0.7
	220.4	−0.1	−0.1	0.1
11	222.3	−1.0	−1.0	−0.1
	222.3	−1.0	−1.0	−0.1
12	221.9	−1.1	−1.1	−0.6
	221.5	−0.7	−0.8	−0.3
13	221.5	−0.8	−0.9	−0.4
	221.5	−0.8	−0.9	−0.4
14	222.0	−0.7	−0.7	0.4
	222.0	−0.7	−0.7	0.3
15	222.8	−1.6	−1.6	−0.8
	222.8	−1.6	−1.6	−0.8
16	223.3	−1.8	−1.9	−0.7
	222.7	−1.5	−1.5	−0.6
17	224.6	−2.8	−2.8	−1.5
	224.6	−2.8	−2.8	−1.5
18	225.2	−3.2	−3.2	−1.5
	223.5	−2.0	−2.0	−0.7
19	215.7	5.6	6.6	6.6
	229.1	−7.8	−6.8	−6.8
20	220.8	−1.8	−1.8	−2.5
	220.8	−1.3	−1.3	−1.7
21	222.6	−1.9	−1.9	−1.9
	222.6	−1.9	−1.9	−1.9
22	223.8	−5.0	−4.2	−4.6
	216.8	1.4	2.3	0.5
23	221.1	−0.4	−0.4	0.2
	221.1	−0.4	−0.4	−0.3
24	221.4	−0.7	−0.7	0.0
	221.4	−0.7	−0.7	0.0
25	221.3	−0.7	−0.7	−0.1
	222.0	−1.3	−1.2	−0.5
26	222.6	−1.2	−1.3	−0.2
	222.9	−1.5	−1.5	−0.4
27	220.4	0.0	0.0	0.1
	220.3	0.0	0.0	0.1
28	223.1	−2.0	−2.0	−1.0
	223.1	−2.0	−2.0	−1.1
29	224.1	−2.3	−1.0	−1.9
	224.4	−2.3	−2.6	−2.4
30	221.8	−1.2	−1.1	−0.5
	221.7	−1.2	−1.2	−0.6
31	221.9	−2.0	−2.0	−2.1
	221.5	−1.7	−1.6	−1.8
32	226.8	−4.2	−4.2	−2.6
	220.0	0.4	0.4	0.7
33	225.3	−2.7	−2.7	−1.1
	222.7	−2.3	−2.3	−2.0

while those that decrease the angle describe rotations away from the central position. The obtained average deviation of 6° is very satisfactory, considering the diversity of the substituents at the π-ligands present in this broad series of examples.

As expected, the lowest torsion angle deviations are found for the very rigid bridged structures. The non-bridged complexes show a tendency to have slightly larger deviations. In the optimized geometries the lateral substituents tend to rotate away from the central position relative to their experimental geometries while the central substituents try to reach the position of highest symmetry.

In those ligands with secondary carbon centers attached to the π-ring, a tendency to larger lateral torsion angles

Table 6. Observed Cl–Zr–Cl Angles and Deviations Obtained in the Force Field Calculations

structure	X-ray value (deg)	Δ (deg) model 1	Δ (deg) model 2	Δ (deg) model 3
1	97.8	−1.5	−1.5	−1.7
2	96.6	0.3	0.3	0.3
3	94.4	1.5	1.5	1.3
4	95.6	0.6	0.6	0.4
5	96.7	−0.5	−0.5	−0.7
6	95.8	1.5	1.5	1.4
7	94.7	2.3	2.3	2.2
8	94.3	1.2	1.2	0.9
9	94.3	2.6	2.6	2.5
10	94.7	2.6	2.6	2.6
11	93.5	1.9	1.9	1.6
12	95.2	0.4	0.4	0.2
13	98.0	−1.8	−1.7	−1.9
14	98.3	0.0	0.0	0.2
15	95.8	0.6	0.6	0.5
16	97.2	−0.9	−0.9	−1.1
17	98.2	1.4	1.6	1.4
19	98.5	−1.1	−1.1	−1.1
20	100.1	−2.2	−2.2	−2.3
21	98.6	−1.6	−1.6	−1.7
22	98.6	−1.4	−1.4	−1.6
23	94.8	−0.8	−0.7	−1.3
24	94.4	−0.2	−0.2	−0.8
25	96.7	−0.9	−0.9	−1.1
26	94.9	1.1	1.1	0.9
27	97.2	0.1	0.1	0.1
28	97.0	−0.1	−0.1	−0.2
29	97.1	−0.5	−0.5	−0.7
31	97.6	−0.5	−0.4	0.2
32	97.3	−0.2	−0.2	−0.3
33	97.2	0.3	0.2	0.2

Table 7. Experimental MP–Zr–MP Angles and Deviations Obtained in the Force Field Calculations

structure	X-ray value (deg)	Δ (deg) model 1	Δ (deg) model 2	Δ (deg) model 3
1	130.0	1.1	1.0	1.2
2	129.1	1.2	1.2	1.2
3	131.0	0.1	0.1	0.1
4	129.9	0.5	0.5	0.5
5	129.7	−0.1	−0.1	0.0
6	130.5	−0.9	−0.9	−0.7
7	131.5	−1.4	−1.5	−1.4
8	128.7	1.7	1.7	1.7
9	133.3	−3.1	−3.1	−3.0
10	129.0	0.6	0.6	0.7
11	128.9	1.7	1.6	1.5
12	130.9	−0.5	−0.5	−0.8
13	130.0	−0.5	−0.4	−0.4
14	129.9	1.6	1.5	1.8
15	130.8	−1.8	−1.8	−1.8
16	130.5	−0.5	−0.5	−0.4
17	134.7	−4.4	−4.5	−4.5
18	131.3	−1.9	−2.0	−1.9
19	130.3	0.0	0.0	0.3
20	130.2	−1.4	−1.3	−1.3
21	127.4	2.6	2.5	0.7
22	118.6	0.0	0.4	0.2
23	127.7	−0.1	0.0	0.3
24	124.8	1.6	1.7	2.1
25	125.2	1.8	1.9	2.0
26	125.2	1.8	1.8	2.0
27	123.9	1.2	1.3	1.2
28	129.6	0.9	0.9	0.8
29	127.2	2.2	2.1	2.2
30	125.8	1.3	1.3	1.5
31	123.8	2.9	3.0	3.0
32	124.4	2.2	2.2	2.5
33	125.0	1.6	1.6	1.9

is found in the X-ray structures (Scheme 1; **4** and **5**). This effect is not reproduced in the optimized geometries. The analysis of the crystal structure for **4**[26] shows close contacts between the substituents of different molecules indicative of crystal-packing effects that cause the extreme position of the ligands.

In the complexes **12** and **13** the lateral substituents are closer to the chlorine atom than in the rest of the structures. In **12**, a complex containing a pair of identical ligands in a bis-lateral arrangement, one substituent is rotated to 110° while the other is located at 99°. This value is also found for the same substituent in structure **4**.[26] This difference cannot be reproduced by the force field calculations and probably has to be attributed to intermolecular interactions in the crystal. The same problem is encountered in complex **20**,[4] where also one torsion angle is increased by 10° with respect to the value for the second (94°) that is also found in the structure **18**.[4]

Complex **14** is a very special case, because the phenyl groups in the substituents are oriented parallel to each other with a distance of about 4.4 Å between the ring planes.[26] In addition, the rings of adjacent molecules form a stack in the crystal structure. This interaction probably causes the observed small torsion angles (60°). The optimized structure reproduces the parallel orientation very well, but the distance between the planes is reduced to 3.4 Å. Thus, in the isolated complex the interaction between the rings is more pronounced and causes a further decrease in the torsion angle about the Zr–MP bonds (45°).

Table 9 summarizes the statistics for the comparison of the experimental structures from X-ray diffraction data with the final optimized structures calculated for the 33 complexes. The statistics show an excellent agreement between the X-ray geometries and the optimized geometries obtained with the three force field models. The ZR entries contain all internal coordinates that involve the metal atom (including the dummy atoms at the center of the π-ligand) and the HEAVY entries all remaining coordinates that do not involve hydrogen atoms. The comparison for all degrees of freedom is given under ALL.

The geometry around the Zr center is rather rigid and can therefore be reproduced to a very high accuracy (1.5 pm and 1°). The small deviations for the heavy atoms show that the substituents are very well represented by the force field and that the potential terms for the metal environment do not introduce additional strain. Intermolecular interactions in the solid state do not cause significant changes in the geometry, except for the special complexes discussed above.

Conclusion

The rigid coordination sphere of the Zr centers facilitates the derivation of force field parameters for the π-ligand complexes. The agreement of the optimized structures obtained with the three models and experimental structural data is excellent. The X-ray structures are well reproduced. Deviations from experimental orientations of some substituents at the π-ligands can easily be rationalized by packing effects in the crystal.

All three force field models developed and tested in this study yield very similar results for the geometries of zirconocene dichlorides. Thus, no extensions to the

(26) Wingbermühle, D.; Erker, G.; Krüger, C.; Nolte, M. Unpublished results.

(27) Erker, G.; Wilker, S.; Krüger, C.; Goddard, R. *J. Am. Chem. Soc.* **1992**, *114*, 10983.

Table 8. Torsion Angles Characterizing the Relative Orientation of the Substituents[a]

structure	S1 (X-ray) (deg)	Δ (deg) model 1	Δ (deg) model 2	Δ (deg) model 3	S2 (X-ray) (deg)	Δ (deg) model 1	Δ (deg) model 2	Δ (deg) model 3	SMMS (deg)	Δ (deg) model 1	Δ (deg) model 2	Δ (deg) model 3
1	180	+1	−1	−1	−144	+2	−2	−3	39	+2	−3	−4
2	−167	−13	−15	−15	−162	−18	−18	−18	34	−34	−34	−34
3	103	+4	+3	+1	−140	−7	−7	−7	−36	−3	−3	+3
4	98	−4	−4	−3	175	+5	+5	+5	−89	+2	+2	+3
5	120	−17	−17	−17	120	−17	−17	−17	−127	−31	−30	−30
6	129	−24	−24	−24	−179	−1	−1	−1	−55	−25	+25	+24
7	−176	−3	−3	−3	−176	−3	−3	−3	8	−7	−7	−7
8	95	−7	−7	−7	95	−7	−7	−7	−174	−11	−11	−10
9	177	+3	+3	+3	177	+3	+3	+3	−7	+7	+7	+7
10	−76	+5	+5	+5	−78	+7	+7	+7	138	+11	+11	+11
11	92	−3	−3	−2	92	−3	−3	−2	180	−3	−3	−2
12	108	−14	−14	−16	98	−4	−4	−4	−159	−14	−14	−13
13	117	−15	−15	−15	117	−15	−15	−15	−133	−25	−25	−25
14	56	−11	−11	−12	59	−14	−14	−15	120	−25	−25	−24
15	89	+5	+5	+4	92	+5	+5	+4	−176	+8	−16	−16
16	93	+5	+5	+5	170	+3	+3	+3	−102	+8	+8	+9
17	93	+2	+2	+2	94	0	+1	+1	−174	+2	+3	+4
18	93	+2	+3	+5	93	+2	+3	+3	−175	+3	+5	+6
19	110	+6	+6	+6	−153	−23	−22	−23	−44	−18	−18	−18
20	105	−6	−6	−6	94	+5	+5	+5	165	0	−1	0
21	179	−4	−4	0	−179	+4	+4	0	0	0	0	0
22	3	−3	0	−3	−3	+3	0	+3	1	−1	0	−1
23	7	−1	−1	0	7	−1	−1	−1	15	−3	−2	−2
24	−8	−3	−9	+1	−8	+13	+9	+16	−18	+5	+5	+4
25	−9	+1	+1	+1	−9	+1	+1	+1	−20	+3	+2	+3
26	19	−2	−2	−2	−4	+1	+1	+2	18	−3	−3	−1
27	−14	−9	−13	−14	21	+6	+12	+12	8	−2	−2	−2
28	−39	+1	+1	+1	40	−2	−2	−2	1	−1	−1	−1
29	−83	+2	+2	+3	50	+5	+6	+6	−31	+7	+7	+8
30	−5	+4	+4	+4	−11	−5	−5	−4	−17	0	0	0
31	−10	+2	+2	−1	−10	+2	+2	+2	−23	+6	+6	+4
32	−5	−4	−4	−2	23	0	0	+1	21	−6	−6	−3
33	2	+7	+7	+5	−15	−8	−8	−7	−10	−5	−5	−8

[a] S1 denotes MP–ZR–MP′–S′, S2 denotes S–MP–ZR–MP′, and SMMS denotes S–MP–MP′–S′.

Table 9. Statistics for a Comparison of Experimental (X-ray and Calculated Force Field Structures for 33 Zirconocene Dichloride Complexes[a]

		model 1		model 2		model 3	
	n	Δ	RMS	Δ	RMS	Δ	RMS
ZR							
bonds	132	1.5	2.1	1.5	2.1	1.4	2.2
angles	198	1.0	0.8	1.0	0.8	1.0	0.8
torsions	990	6.3	6.0	6.3	6.1	6.2	6.1
HEAVY							
bonds	1271	1.9	1.9	1.9	2.0	1.8	1.9
angles	3105	1.2	1.4	1.2	1.4	1.1	1.3
torsions	5438	2.7	4.3	2.7	4.0	2.5	4.1
ALL							
bonds	2453	1.1	1.8	1.1	1.7	1.1	1.7
angles	5822	1.0	1.1	1.0	1.1	0.9	1.1
torsions	10658	3.3	5.3	3.3	5.1	3.2	5.0

[a] *n* gives the numbers of geometry parameters; Δ denotes the deviation for the bond length (pm), bond angles (deg), and torsion angles (deg).

existing force field implementations (model 1) are needed to describe the static properties of π-ligand complexes with accuracy similar to that for organic compounds. The additional parameters presented here for model 1 can be used with most commercial modeling packages. Our calculations on four representative complexes using the parameters derived here for the AMBER-type force field within the TRIPOS 5.2 parametrization[13] support this high transferability.[28]

Neither model 1 nor model 2 needs extraordinarily high force constants for the valence force field terms that couple the dummy atom to the π-system. The vibrations involving the dummy atoms in models 1 and 2 do not effect the "real" vibrations of the molecule. The calculated IR spectra are not affected by these spurious vibrations. Thus, the two models may also be applied to study the dynamic behavior of such zirconocene complexes.

The accuracy of the structural description of Cp-substituted zirconocene dichlorides and analogues is very satisfactory and will allow a more detailed investigation of the structures and properties of π-ligand metal complexes. Our study is currently extended to dialkylzirconocene derivatives and modeling of Ziegler–Natta catalysts. The parametrization of other early-transition-metal complexes is under way.[29] Preliminary results for the rotameric distribution and the dynamic properties of zirconocene dichloride complexes are in good agreement with the experimental findings obtained by dynamic NMR measurements and will be reported elsewhere.[20]

(28) We do not explicitly give the results for these calculations because they agree with those given in Tables 6–8.

(29) Höweler, U.; Knickmeier, M.; Mohr, R.; Erker, G. Manuscript in preparation.

(30) 1: Rogers, R. G.; Benning, M. M.; Kurihara, L. K.; Moriarty, K. J.; Rausch, M. D. *J. Organomet. Chem.* **1985**, *293*, 51. 2: Erker, G.; Nolte, R.; Tsay, Y.-H.; Krüger, C. *Angew. Chem.* **1989**, *101*, 642; *Angew. Chem., Int. Ed. Engl.* **1989**, *29*, 628. 3, 11: Dehnicke, S.; Erker, G.; Krüger, C.; Angermund, K. Unpublished results. 4: Reference 26. 5–7: Krüger, C.; Nolte, M.; Erker, G.; Thiele, S. *Z. Naturforsch.* **1992**, *47B*, 995. 8: Howie, R. G.; McQuillan, G. P.; Thompson, D. W.; Lock, G. A. *J. Organomet. Chem.* **1986**, *303*, 213. 9: Dusausoy, Y.; Protas, J.; Renaut, P.; Gautheron, B.; Tainturier, G. *J. Organomet. Chem.* **1978**, *157*, 167. 10: Gallucci, J. C.; Gautheon, B.; Gugelchuk, M.; Meunier, P.; Paquette, L. A. *Organometallics* **1987**, *6*, 15. 11: Reference 25. 12: Cesarotti, E.; Kagan, H. B.; Goddart, R.; Krüger, C. *J. Organomet. Chem.* **1978**, *162*, 297. 13: Erker, G.; Nolte, R.; Aul, R.; Wilker, S.; Krüger, C.; Noe, R. *J. Am. Chem. Soc.* **1991**, *113*, 7594. 14, 21: Reference 27. 15, 16: Krüger, C.; Lutz, F.; Nolte, M.; Erker, G.; Aulbach, M. *J. Organomet. Chem.* **1993**, *452*, 79. 17–20: Reference 4.

Acknowledgment. Financial support from the Fonds der Chemischen Industrie and the Alfried Krupp von Bohlen und Halbach-Stiftung is gratefully acknowledged. We also thank Prof. Dr. C. Krüger, Dr. K. Angermund, and Dr. M. Nolte at the Max-Planck-Institut für Kohlenforschung in Mülheim a.d. Ruhr, Germany, for stimulating discussions.

Supplementary Material Available: Listings giving the Cartesian coordinates of the X-ray diffraction data, the optimized structures (**1–33**), and a complete parameter file (MOBY format, ASCII) (350 pages). Ordering information is given on any current masthead page. This material may also be obtained by sending an empty PC diskette to U.H.

OM940145C

(31) **22**: Razavi, A.; Ferrara, J. *J. Organomet. Chem.* **1992**, *435*, 299. **23**: Wochner, F.; Zsolnai, L.; Huttner, G.; Brintzinger, H. H. *J. Organomet. Chem.* **1985**, *288*, 69. **24, 31**: Gutmann, S.; Burger, P.; Hund, H.-U.; Hofmann, J.; Brintzinger, H. H. *J. Organomet. Chem.* **1989**, *369*, 343. **25–26**: Collins, S.; Kuntz, B. A.; Taylor, N. J. Ward, D. G. *J. Organomet. Chem.* **1988**, *342*, 21. **27**: Erker, G.; Nolte, R.; Aul, R.; Wilker, S.; Krüger, C.; Noe, R. *J. Am. Chem. Soc.* **1991**, *113*, 7594. **28**: Saldarriaga-Molna, C. H.; Clearfield, A.; Bernal, I. *J. Organomet. Chem.* **1974**, *80*, 79. **29**: Green, M. L. H.; Gardinier, I. M.; Brandy, J. A.; Prout, K. *J. Chem. Soc., Dalton Trans.* **1991**, 2207. **30**: Rheingold, A. L.; Robinson, N. P.; Whelan, J.; Bosnich, B. *Organometallics* **1992**, *5*, 1869. **32, 33**: Rieger, B.; Steimann, M.; Fazawi, R. *Chem. Ber.* **1992**, *125*, 2373.

(32) Fritz, H. P. *Advances in Organometallic Chemistry*; Academic Press: New York, 1964; p 262.